

Titanium Dioxide Nanoparticles Induce Cognitive Dysfunction of Rats with Endogenous Protective Mechanism of Increased miR-21-5p

Chao Li

Tianjin Institute of Environmental and Operational Medicine

Fei Wei

Binzhou Medical University

Chengfeng Shen

Tianjin Centers for Disease Control and Prevention

Xiaoming Wang

Tianjin Institute of Environmental and Operational Medicine

Xiujie Gao

Tianjin Institute of Environmental and Operational Medicine

Zhaoli Chen

Tianjin Institute of Environmental and Operational Medicine

Tie Han

Tianjin Institute of Environmental and Operational Medicine

Xinxing Wang (✉ wxxemail@sina.cn)

Tianjin Institute of Environmental and Operational Medicine <https://orcid.org/0000-0003-1650-3297>

Research

Keywords: Titanium dioxide nanoparticle, cognitive deficits, mitochondria, voltage-dependent anion channel 1, microRNA-21-5p

Posted Date: January 15th, 2021

DOI: <https://doi.org/10.21203/rs.3.rs-144989/v1>

License: © ⓘ This work is licensed under a Creative Commons Attribution 4.0 International License.

[Read Full License](#)

Abstract

Background

Titanium dioxide nanoparticles (TiO₂ NPs) cause nerve cell damage and central nervous system dysfunction has been well known. However, most of the cognitive deficits occurs before the observable damage to nerve cells and the regulatory mechanism is largely unknown. Mitochondria and energy metabolism are the targets of many neurotoxic substances.

Results

Here, we showed that TiO₂ NPs exposure reduced the mitochondrial membrane potential ($\Delta\Psi_m$) and ATP content, which is the important cause of cognitive deficits, and upregulated microRNA-21-5p (miR-21-5p) levels in rat neuron cells. Upregulated miR-21-5p promoted phosphorylation of c-Jun, consequently promoting transcription of *VDAC1* (encoding voltage-dependent anion channel 1), which in turn preserved the $\Delta\Psi_m$ and ATP content of neuron cells.

Conclusions

Mechanistically, upregulated *VDAC1* was attributed to TiO₂ NPs-induced phosphorylation of c-Jun (Ser73), which is predicted to be a transcription factor of *VDAC1*, while upregulation of the $\Delta\Psi_m$ and ATP content was caused by the increased oxygen consumption rate induced by *VDAC1*. The results of our present study revealed an endogenous self-protection mechanism in the process of TiO₂ NPs-induced cognitive deficits.

1. Introduction

Titanium dioxide nanoparticles (TiO₂ NPs) have high chemical stability, and excellent optical properties, thus are used widely in various fields, such as cosmetics production, food processing, paint manufacturing, etc. [1]. TiO₂ has been approved by the US Food and Drug Administration for food production as a color additive many years ago [2, 3]. It has been reported that over 93% of the TiO₂ in gum comprises TiO₂ NPs [2]. TiO₂ NPs also has been found in many foods that claim not to contain TiO₂ NPs, and previous tests have shown up to 9 g/kg of food [4]. There is increasing awareness of the health risks caused by the absorption of TiO₂ NPs into the human body. The central nervous system (CNS) is one of the important targets for TiO₂ NPs [5]. The digestive system is an important way for TiO₂ NPs to enter the human body. After entering the blood through the digestive tract, TiO₂ NPs can enter the central nervous system through the blood-brain barrier due to its small size [6, 7], where they damage nerve cell function by promoting inflammation, activating oxidative stress, and destroying cell membrane [8].

It has been reported that TiO₂ NPs induced inflammatory injury in SH-SY5Y cells (Cells derived from human bone marrow neuroblastoma) in a dose-dependent manner [5]. *In vivo*, TiO₂ NPs entering the

central nervous system (CNS) can lead to mitochondrial dysfunction and decrease of mitochondrial membrane potential ($\Delta\Psi_m$) [9]. In the CNS, the energy metabolism level determines the brain's ability to perform its normal functions, such as learning and memory [10, 11]. It has been reported that TiO_2 NPs could cause $\Delta\Psi_m$ loss, hippocampal damage, and impairment of spatial recognition memory in mice, which indicated that TiO_2 NPs promote apoptosis of hippocampal neurons through the mitochondrial pathway [12]. So far, dysfunction of the central nervous system is believed to be the result of neuronal cell damage induced by TiO_2 NPs, which promote energy metabolism disorders. However, most of the central nervous system dysfunction occurs before the observable damage to nerve cells. This means that when the damaging effect is observed, the best time to prevent it has been missed. Therefore, revealing the molecular mechanism of TiO_2 NPs-induced energy metabolism disorder will help to prevent the damaging effect of the nervous system earlier.

Our present study defined a novel mechanism of energy metabolism damaged by TiO_2 NPs in neuron cells. Upregulated miR-21-5P, induced by TiO_2 NPs, preserved TiO_2 NPs-induced the decline of $\Delta\Psi_m$ and ATP content through increasing oxygen consumption rate (OCR). Upregulation of miR-21-5P promoted transcription of *VDAC1* (encoding voltage-dependent anion channel 1) leading to the upregulation of VDAC1 protein levels, which in turn preserved the OCR, $\Delta\Psi_m$, and ATP content of neuron cells under TiO_2 NPs exposure. This endogenous self-protection mechanism in the process of TiO_2 NPs-induced energy metabolism disorder in neuron cells could improve our understanding of TiO_2 NPs-induced nervous system dysfunction and help us to prevent TiO_2 NPs-induced CNS injury earlier.

2. Materials And Methods

2.1 Animals and treatments

This study was conducted with the approval of the Animal Care and Use Committee of the Tianjin Institute of Environmental and Operational Medicine, China. All rats handling procedures were performed in strict accordance with the guide for the use and care of laboratory animals. All surgery was performed under sodium pentobarbital (1%, 1 mL/100 g weight, i.p.) anesthesia.

Before the experiment, male Wistar rats (180–200 g) were kept in their surroundings for 1 week. The rats were maintained on a 12 h light/dark cycle in constant temperature environment (25 ± 2 °C). Animals were randomly divided into four groups: Control group (treated with 0.5% w/v hydroxypropyl methylcellulose (HPMC)) and three experimental groups (10, 20, or 30 mg/kg body weight (BW) TiO_2 NPs). The TiO_2 NPs (Sigma-Aldrich, St. Louis, MO, USA; 637254) suspensions were given to the rats via intragastric administration every day for 4, 6, or 8 weeks, respectively. Animals were weighed before intragastric administration every day.

The water maze was used to test cognitive function as previously reported [13]. The test was conducted three times a session for 4 consecutive days with an interval of 30 minutes. Software (v3.1.16 Noldus

Information Technology, Wageningen, Netherlands. Statsoft Inc. Oklahoma, USA) was used to track the swimming path in each test.

2.2 Cell culture, Constructs, Reagents, Antibodies, and Quantitative Real-Time PCR (qPCR)

Please refer to the supplementary materials for details

2.3 Mitochondrial membrane potential ($\Delta\Psi_m$)

JC-1 (5,5',6,6'-Tetrachloro-1,1',3,3'-tetraethyl-imidacarbocyanine iodide, Sigma-Aldrich) was used to detect the $\Delta\Psi_m$. Cells were placed in a culture medium containing JC-1 (2.5 $\mu\text{g}/\text{mL}$) for 30 min in a cell incubator. Flow cytometry (FCM) was used to detect the $\Delta\Psi_m$.

2.4 ATP content

Cold phosphate-buffered saline (PBS) was used to collect cells, and the samples were quickly frozen and preserved in liquid nitrogen. The samples were melted slowly in an ice water bath and vortexed for 10 s. Luciferase driven bioluminescence with an ATP Bioluminescence Assay Kit HS II (Sigma-Aldrich, Cat. No. 11699709001) was used to assay the ATP content.

2.5 Seahorse

The OCR and ECAR were measured as described previously [14] using a Seahorse XFe24 system (Agilent Technologies, Santa Clara, CA, USA).

2.6 Luciferase Reporter Assay

Luciferase reporter assays were conducted as previous reports [15].

2.7 Western Blotting

Western blotting was conducted as described in our previous publication [16].

2.8 Statistical Analysis

SPSS 17.0 software (IBM Corp., Armonk, NY, USA) was used to perform statistical analyses. The differences between two groups were determined using Student's t-test. For three and more groups of data, statistical analysis was performed using analysis of variance (ANOVA) followed by the Tukey-Kramer multiple comparisons test or an unpaired two-tailed Student-t-test. A *P* value less than 0.05 was considered statistically significant.

3. Results

3.1 Upregulation of miR-21-5P expression, mitochondrial dysfunction and cognitive deficits were observed in response to TiO₂ NPs.

As shown in Fig. 1, increased levels of miR-21-5P were detected in prefrontal cortex of rat (Fig. 1A & 1D), primary neuron cells (Fig. 1B & 1E), and SH-SY5Y cells (Fig. 1C & 1F) in response to TiO₂ NPs. The prefrontal cortex requires a large amount of energy, and multiple information processing functions, such as memory, judgment, analysis and thinking, which are involved in preserving fundamental cognitive ability, require energy in the form of ATP. Regulation of the energy balance might be a key factor involved in neuroprotection against TiO₂ NPs. Thus, we determined the $\Delta\Psi_m$ and ATP content and found that the $\Delta\Psi_m$ and ATP levels decreased markedly in response to TiO₂ NPs in a dose-dependent manner (Fig. 1G & 1H). Water maze test showed that the latency of rats to locate the hidden platform was significantly prolonged after titanium dioxide intervention (Fig. 1I). Meanwhile, the swimming distance of rats at the edge of the pool was also significantly increased (Fig. 1J & 1K). These results suggested that miR-21-5p might be related to mitochondrial function and cognitive deficits under TiO₂ NP treatment.

3.2 MiR-21-5p preserves the $\Delta\Psi_m$ and ATP levels of SH-SY5Y cells under TiO₂ NP treatment.

It has been reported that intracellular reactive oxygen species (ROS) can regulate miR-21-mediated pathways [17, 18]; however, regulation by miR-21 of mitochondrial function is rarely reported. To further explore the relationship between miR-21-5p and mitochondrial function under TiO₂ NP intervention, we analyzed the correlation between miR-21-5p and the $\Delta\Psi_m$ in SH-SY5Y cells treated with TiO₂ NPs. The results showed that the level of miR-21-5p correlated significantly with the $\Delta\Psi_m$ in SH-SY5Y cells treated with TiO₂ NPs (Fig. 2A). There was also a significant positive correlation between the ATP content and miR-21-5p levels in TiO₂ NPs-treated SH-SY5Y cells (Fig. 2B). These results suggested that miR-21-5p has a protective effect on mitochondrial function in SH-SY5Y cells treated with TiO₂ NPs. An miR-21-5p overexpression vector (Fig. 2C) and short hairpin RNA (shRNA) vector to silence miR-21-5p (Fig. 2D) were employed to further evaluate the protective effect of miR-21-5p on mitochondrial function in SH-SY5Y cells treated with TiO₂ NPs. As shown in Fig. 2E, knockdown of miR-21-5p by shmiR-21-5p led to a further decrease in the $\Delta\Psi_m$ of TiO₂ NPs-treated SH-SY5Y cells, and miR-21-5p overexpression reversed the decrease in the $\Delta\Psi_m$ induced by TiO₂ NPs. Furthermore, miR-21-5p overexpression reversed the decrease in the ATP content induced by TiO₂ NPs in SH-SY5Y cells (Fig. 2F). These results demonstrated that miR-21-5p protects mitochondrial function against damage from TiO₂ NPs in SH-SY5Y cells.

3.3 MiR-21-5p protects the respiratory and glycolytic ability of cells under TiO₂ NPs treatment.

To further assess the effects of miR-21-5p on energy metabolism function in SH-SY5Y cells, the oxygen consumption rate (OCR) and extracellular acidification rate (ECAR) of SH-SY5Y cells were measured by Seahorse XF-24 system (Fig. 3A). All data were normalized to ensure that they were not affected by cell density [14]. Basal, ATP-linked, and maximal respiration were significantly decreased in miR-21-5p-

silenced SH-SY5Y cells (shmiR-21-5p) compared with those in the controls (Fig. 3B). The inhibition of ATP-linked respiration and decline of ATP content mentioned in Fig. 2F showed the same trend. In order to further observe the effect of m on cell glycolysis activity, ECAR induced by oligomycin was employed [19, 20]. A remarkably decrease in ECAR induced by oligomycin was detected in miR-21-5p-silenced SH-SY5Y cells (shmiR-21-5p) compared with that in the controls under TiO₂ NPs treatment. No difference between groups was observed in basal ECAR (Fig. 3C). The OCR to ECAR ratio showed decreased induction of respiratory capacity in miR-21-5p-silenced SH-SY5Y cells (shmiR-21-5p) compared with that in the controls (Fig. 3D). These results indicated that miR-21-5p protects the ability of SH-SY5Y cells to respond to TiO₂ NPs.

3.4 VDAC1 is crucial for miR-21-5p in protecting the mitochondria function of SH-SY5Y cells in response to TiO₂ NPs.

The voltage-dependent anion channel 1 (VDAC1) locates in mitochondrial outer membrane, where it regulates protein and metabolite trafficking in and out of the mitochondria [21]. It has also been reported that VDAC has an important relationship with mitochondrial respiration [22]. Thus, we assessed the levels of VDACS, including VDAC1, VDAC2, and VDAC3, in SH-SY5Y cells with or without shmiR-21-5p. As shown in Fig. 4A, VDAC1 and VDAC3 levels decreased markedly in SH-SY5Y cells (shmiR-21-5p) compared with those in SH-SY5Y cells (Nonsense) under TiO₂ NPs treatment. The level of VDAC1 increased significantly in response to TiO₂ NPs treatment, while VDAC3 levels were similar between the groups (Fig. 4B). A *VDAC1* overexpression vector (Fig. 4C) was employed to study the role of VDAC1 in miR-21-mediated protection of respiratory function in response to TiO₂ NPs treatment. *VDAC1* overexpression reversed the lower $\Delta\Psi_m$ levels (Fig. 4D) and ATP content (Fig. 4E) induced by shmiR-21-5p under TiO₂ NPs treatment. Similarly, *VDAC1* overexpression increased the basal, ATP-linked, and maximal respiration that had been decreased by shmiR-21-5p in SH-SY5Y cells under TiO₂ NPs treatment (Fig. 4F). These results confirmed that VDAC1 plays an important role in mir-21-5p-mediated protection of cellular respiratory function

3.5 Phosphorylated c-Jun is responsible for *VDAC1* upregulation.

The mRNA levels of *VDAC1* in TiO₂ NPs-treated SH-SY5Y cells were remarkably higher than those in the control group (Fig. 5A). Overexpression of miR-21-5p resulted in a significantly higher level of *VDAC1* mRNA under TiO₂ NPs treatment (Fig. 5B), while knockdown of miR-21-5p by shmiR-21-5p decreased the *VDAC1* mRNA level compared with that in control group (Fig. 5C). These results suggested that miR-21-5p regulates the transcription of *VDAC1*. To study the molecular mechanism by which miR-21-5p regulates *VDAC1* transcription, *VDAC1* promoter constructs Del 1 (-2000 to +135) and Del 2 (-908 to +135) (Fig. 5D) were employed to assess promoter-dependent transcriptional activity. The promoter-dependent transcriptional activity of the *VDAC1* promoter construct Del 1 was remarkably higher in TiO₂ NPs-treated SH-SY5Y cells than in the control group, while the activity of *VDAC1* promoter construct Del 2 was not different between the groups (Fig. 5E). Thus, TiO₂ NPs may increase the mRNA levels of *VDAC1* through

the promoter region (-2000 to -908). Next, potential transcription factors were predicted and detected by western blotting. The results indicated that TiO₂ NPs promoted the phosphorylation of c-jun, but had no effect on other transcription factors, including c-ETS1, T3R-β, c-Myb, and NF-AT2 (Fig. 5G). Inhibition of c-Jun phosphorylation prevented the transcription of *VDAC1* mRNA (Fig. 5H) under TiO₂ NPs treatment and led to a further decline in the ΔΨ_m level (Fig. 5I) and ATP (Fig. 5J) content in SH-SY5Y cells. These results suggested that phosphorylated c-Jun, as a transcription factor of *VDAC1*, promotes the transcription of *VDAC1* mRNA and protects the respiration function in SH-SY5Y cells under TiO₂ NPs treatment. Taken together, our results strongly demonstrated that miR-21-5p upregulation contributes to TiO₂ NPs-induced c-Jun (Ser73) phosphorylation, which, as a transcription factor, leads to *VDAC1* transcriptional upregulation, which in preserves the ΔΨ_m level and ATP content in neuron cells, as summarized in Graphical abstract.

4. Discussion

Titanium dioxide nanoparticles (TiO₂ NPs) have been widely used in various industries, such as chemistry, paint, food, and medicine [23]. It has been reported that TiO₂ NPs induce central nervous system (CNS) dysfunction by accumulating in the brain [24]. In zebrafish, a low dose of TiO₂ NPs (5 μg/L) can lead to the aggregation of TiO₂ NPs in neurons, the increase of apoptosis, and the decrease of spatial recognition [25]. *In vitro*, TiO₂ NPs were also found to induce apoptosis in primary cultured hippocampal neurons [12]. In the process of TiO₂ NPs-induced neuron apoptosis, it was found that TiO₂ NPs could promote the decrease of ΔΨ_m, the release of cytochrome c, and the increase of caspase-3 level [24]. Those results indicated that mitochondria participate in the apoptosis of neurons induced by TiO₂ NPs. Mitochondria are semi-autonomous organelles responsible for energy production, cell differentiation, cell information transmission, cell growth, and cell cycle [26]. Given their many crucial functions in cell physiology, it is not surprising that mitochondria are involved in, or mediate, cognitive deficits, even before neuronal damage. Although some studies have reported the damaging effect of TiO₂ NPs on mitochondrial function, to date, most studies have focused on the downstream signaling pathway after mitochondrial function damage, such as the activation of the apoptosis pathway or oxidative stress effects. The molecular mechanisms of mitochondrial function regulation under the influence of TiO₂ NPs remain unclear. Understanding these mechanisms is essential to protect CNS function under TiO₂ NPs exposure. In the present study, we demonstrated that TiO₂ NPs are strong positive regulators of miR-21-5p expression, which protects the neuron cells in response to TiO₂ NPs, and that *VDAC1* plays an important role in the function of miR-21-5p by preserving oxygen consumption rate, ΔΨ_m, and the ATP content.

MiR-21 is considered an oncogenic molecular due to inhibiting the expression of phosphatases, which regulate the signaling pathways such as AKT and MAPK in cells [27, 28]. In non-cancer cells, miR-21 usually acts as a protector [29, 30, 31]. Although microRNA-21 (miR-21) is believed to be related to the regulation of mitochondrial energy metabolism [32, 33, 34, 35], the effect of TiO₂ NPs on miR-21 has not

been reported. In the present study, we discovered that the level of miR-21-5p was upregulated in primary neuron cells, SH-SY5Y cells, and rat prefrontal cortex under TiO₂ NPs treatment in a dose- and time-dependent manner (Fig. 1A – 1F). Considering that TiO₂ NPs also led to a decrease in the $\Delta\Psi_m$ (Fig. 1G) and ATP content (Fig. 1H), miR-21-5p seemed to be a cause or result of mitochondrial dysfunction under TiO₂ NPs treatment. To confirm the function of miR-21-5p, the correlation of the miR-21-5p level with the $\Delta\Psi_m$ or ATP content of SH-SY5Y cells treated with TiO₂ NPs was analyzed, and SH-SY5Y cells (miR-21) and SH-SY5Y cells (shmiR-21) were employed (Fig. 2C & 2D). Under TiO₂ NPs treatment, there was a significant correlation between miR-21-5p and the $\Delta\Psi_m$ (Fig. 2A) or the ATP content (Fig. 2B). Knockdown of miR-21-5p resulted in a significant decrease in the $\Delta\Psi_m$ and ATP content of SH-SY5Y cells under TiO₂ NPs treatment. Overexpression of miR-21-5p resulted a significant increase in the $\Delta\Psi_m$ and ATP content of SH-SY5Y cells under TiO₂ NPs treatment (Fig. 2E & 2F). Our results indicated that the increase of miR-21-5p expression induced by TiO₂ NPs is an important protective mechanism to preserve the $\Delta\Psi_m$ and ATP content in neuron cells.

In the process of mitochondrial electron transport, the electrochemical potential energy is stored in the inner membrane of mitochondria. On both sides of the inner membrane, the asymmetric distribution of proton and other ion concentration will form the $\Delta\Psi_m$, which is the core driving oxidative phosphorylation to produce ATP [36]. The oxygen consumption rate (OCR) is the basis of mitochondrial oxidative phosphorylation and ATP synthesis [14, 37]. In our study, OCR was measured using the Seahorse system in SH-SY5Y cells (shmiR-21) and SH-SY5Y cells (Nonsense) under TiO₂ NPs treatment. Basal, ATP-linked, and maximal respiration were remarkably declined in SH-SY5Y cells (shmiR-21) compared with those in SH-SY5Y cells (Nonsense) (Fig. 3B). This inhibition in ATP-linked respiration corresponded with the decreased ATP content in SH-SY5Y cells (shmiR-21) (Fig. 2F). Thus the damaged OCR induced by TiO₂ NPs was protected by miR-21-5p. Although glycogen depletion, caused by uncontrolled glycolysis, leads to cognitive impairment [38], glycolysis is the main source of energy supply for anoxic neurons. Moreover, previous studies suggested that lactate, a glycolytic product, plays an important role in memory processing [14]. Our results showed that miR-21 knockdown reduced the extracellular acidification rate (ECAR) induced by oligomycin under TiO₂ NPs treatment (Fig. 3C). This suggested that glycolysis is also one of the ways by which miR-21 protects neurons under TiO₂ NPs treatment.

Voltage-dependent ion channels are involved in the process of energy metabolism [39]. Here, we determined the expression levels of VDACs, and found that VDAC1 expression was regulated by miR-21 (Fig. 4A) as well as by TiO₂ NPs (Fig. 4B). VDAC1 plays an important role in glycolysis and oxidative phosphorylation [40]. High levels of VDAC1 were demonstrated in the brains of patients with Alzheimer's disease and in amyloid precursor protein transgenic mice [41]. Some studies have found that Vdac1 overexpression is related to the release of cytochrome c [40]. However, in the present study, VDAC1 overexpression reversed the reduction of the $\Delta\Psi_m$ (Fig. 4D) and ATP content (Fig. 4E) induced by miR-21 knockdown in SH-SY5Y cells under TiO₂ NPs treatment. Basal, ATP-linked, and maximal respiration also increased significantly in SH-SY5Y cells (VDAC1, shmiR-21) compared with those in control SH-SY5Y

cells (Vector, shmiR-21) (Fig. 4F). Therefore, we speculated that TiO₂ NPs would upregulate the VDAC1 via miR-21 accumulation, which, as an endogenous protection mechanism, consequently preserves the OCR, $\Delta\Psi_m$, and ATP content.

Up to now, no mechanism of titanium dioxide regulating VDAC has been reported. To explore how miR-21 regulates VDAC1 under TiO₂ NPs treatment, we detected the *VDAC1* mRNA level in SH-SY5Y, SH-SY5Y (miR-21), and SH-SY5Y (shmiR-21) cells with TiO₂ NPs treatment (Fig. 5A – 5C). Thus, miR-21 might upregulate the VDAC1 by promoting its mRNA transcription under TiO₂ NPs treatment. To verify this speculation, the promoter-dependent transcriptional activities of *VDAC1* were detected in SH-SY5Y cells with or without TiO₂ NPs treatment. The results indicated that *VDAC1* promoter transcription factor binding sites (-908 to -2000) were responsible for *VDAC1* mRNA upregulation in TiO₂ NPs-treated cells (Fig. 5D & 5E). Although studies have reported that the transcriptional regulation of *VDAC1* plays an important role in different cell models [42, 43, 44], the mechanism of *VDAC1* transcription regulation is still unclear, especially under the intervention of TiO₂ NPs. Bioinformatic methods predicted transcription factor binding sites and then the levels of the predicted transcription factors using western blotting in cells with or without TiO₂ NPs treatment (Fig. 5G). The level of phosphorylated (P)-c-Jun (Ser73) was upregulated markedly in TiO₂ NPstreated SH-SY5Y cells compared with that in the control cells. Furthermore, inhibition of c-Jun phosphorylation reversed the upregulation of VDAC1 induced by TiO₂ NPs and decreased the $\Delta\Psi_m$ and ATP content in SH-SY5Y cells. Based on these results, we proposed a previously unreported mechanism of *VDAC1* transcriptional regulation and the protective role of VDAC1 protein in neuron cells in response to TiO₂ NPs.

In summary (Graphical abstract), our results defined a novel effect of TiO₂ NPs on miR-21-5p upregulation, which would inhibit the expression of an as yet unidentified phosphatase, leading to increased or maintained phosphorylation of c-Jun. This active form of c-Jun would increase the transcriptional activity of *VDAC1* leading to the upregulation of VDAC1 protein levels, an increased OCR, elevation of the $\Delta\Psi_m$, and preservation of the ATP content. These findings demonstrated the protective of miR-21 in TiO₂ NPs-induced neuron cells, providing novel insights into the multiple levels of VDAC1 protein regulation and revealed an endogenous neuroprotective mechanism in response to TiO₂ NPs.

5. Conclusion

TiO₂ is widely used in the processing of food, medicine, and cosmetics. Most products claim to contain TiO₂ NPs free. However, TiO₂ NPs has been found in a variety of products. In the present study, we found that TiO₂ NPs leads to cognitive decline by declining the oxygen consumption rate and ATP level of neurons. Downregulated VDAC1 is responsible for declined energy metabolism induced by TiO₂ NPs. Up-regulation of miR-21-5p may be one of the endogenous protective mechanisms of TiO₂ NPs injury by preserving energy metabolism of neurons. This study provides new evidence for TiO₂ NPs-induced nervous system injury.

6. Declarations

Ethics approval and consent to participate

This study was compliant with the Declaration of Helsinki Guidelines and was approved by the Committee on the Ethics of Animal Experiments of the Tianjin Institute of Environmental and Operational Medicine.

Consent for publication

Not applicable.

Availability of data and materials

All data generated or analyzed during this study are included in this published article.

Competing interests

The authors declare that they have no competing interests.

Funding

This work was partially supported by the grants from the National Natural Science Foundation of China [grant numbers 31971106, 81372124].

Authors' contributions

Conception and design: Xinxing Wang. Acquisition of data (acquired and managed patients, provided facilities, etc.): Chao Li, Fei Wei, and Xiujie Gao, Xiaoming Wang. Analysis and interpretation of data (e.g., statistical analysis, biostatistics, and computational analysis): Chengfeng Shen, and Tie Han. Writing, review, and/or revision of the manuscript: Chao Li, Xinxing Wang, and Tie Han. Administrative, technical, or material support (i.e., reporting or organizing data, constructing databases): Fei Wei, Chao Li, and Xinxing Wang. Study supervision: Xinxing Wang, Tie Han and Zhaoli Chen.

Acknowledgements

Not applicable.

7. References

1. Shakeel M, Jabeen F, Shabbir S, Asghar MS, Khan MS, Chaudhry AS. Toxicity of Nano-Titanium Dioxide (TiO₂-NP) Through Various Routes of Exposure: a Review. *Biological trace element research*. 2016;172 1:1-36; doi: 10.1007/s12011-015-0550-x. <http://www.ncbi.nlm.nih.gov/pubmed/26554951>.
2. Chen XX, Cheng B, Yang YX, Cao A, Liu JH, Du LJ, et al. Characterization and preliminary toxicity assay of nano-titanium dioxide additive in sugar-coated chewing gum. *Small*. 2013;9 9-10:1765-74;

- doi: 10.1002/sml.201201506. <http://www.ncbi.nlm.nih.gov/pubmed/23065899>.
3. Grissa I, ElGhoul J, Mrimi R, Mir LE, Cheikh HB, Horcajada P. In deep evaluation of the neurotoxicity of orally administered TiO₂ nanoparticles. *Brain research bulletin*. 2020;155:119-28; doi: 10.1016/j.brainresbull.2019.10.005. <http://www.ncbi.nlm.nih.gov/pubmed/31715315>.
 4. Jia X, Wang S, Zhou L, Sun L. The Potential Liver, Brain, and Embryo Toxicity of Titanium Dioxide Nanoparticles on Mice. *Nanoscale research letters*. 2017;12 1:478; doi: 10.1186/s11671-017-2242-2. <http://www.ncbi.nlm.nih.gov/pubmed/28774157>.
 5. Zhou T, Huang WK, Xu QY, Zhou X, Wang Y, Yue ZH, et al. Nec-1 Attenuates Neurotoxicity Induced by Titanium Dioxide Nanomaterials on Sh-Sy5y Cells Through RIP1. *Nanoscale research letters*. 2020;15 1:65; doi: 10.1186/s11671-020-03300-5. <http://www.ncbi.nlm.nih.gov/pubmed/32221753>.
 6. Kwon S, Yang YS, Yang HS, Lee J, Kang MS, Lee BS, et al. Nasal and pulmonary toxicity of titanium dioxide nanoparticles in rats. *Toxicological research*. 2012;28 4:217-24; doi: 10.5487/TR.2012.28.4.217. <http://www.ncbi.nlm.nih.gov/pubmed/24278613>.
 7. Swidwinska-Gajewska AM, Czerczak S. Titanium dioxide nanoparticles–biological effects. *Medycyna pracy*. 2014;65 5:651-63. <http://www.ncbi.nlm.nih.gov/pubmed/25812394>.
 8. Wu T, Tang M. The inflammatory response to silver and titanium dioxide nanoparticles in the central nervous system. *Nanomedicine*. 2018;13 2:233-49; doi: 10.2217/nnm-2017-0270. <http://www.ncbi.nlm.nih.gov/pubmed/29199887>.
 9. Perez-Arizti JA, Ventura-Gallegos JL, Galvan Juarez RE, Ramos-Godinez MDP, Colin-Val Z, Lopez-Marure R. Titanium dioxide nanoparticles promote oxidative stress, autophagy and reduce NLRP3 in primary rat astrocytes. *Chemico-biological interactions*. 2020;317:108966; doi: 10.1016/j.cbi.2020.108966. <http://www.ncbi.nlm.nih.gov/pubmed/32004531>.
 10. Jang Y, Lee JH, Lee MJ, Kim SJ, Ju X, Cui J, et al. Schisandra Extract and Ascorbic Acid Synergistically Enhance Cognition in Mice Through Modulation of Mitochondrial Respiration. *Nutrients*. 2020;12 4; doi: 10.3390/nu12040897.
 11. Yamada Y, Nishii K, Kuwata K, Nakamichi M, Nakanishi K, Sugimoto A, et al. Effects of pyrroloquinoline quinone and imidazole pyrroloquinoline on biological activities and neural functions. *Heliyon*. 2020;6 1:e03240; doi: 10.1016/j.heliyon.2020.e03240.
 12. Sheng L, Ze Y, Wang L, Yu X, Hong J, Zhao X, et al. Mechanisms of TiO₂ nanoparticle-induced neuronal apoptosis in rat primary cultured hippocampal neurons. *Journal of biomedical materials research Part A*. 2015;103 3:1141-9; doi: 10.1002/jbm.a.35263. <http://www.ncbi.nlm.nih.gov/pubmed/25045142>.
 13. Callaway JK, Jones NC, Royse CF. Isoflurane induces cognitive deficits in the Morris water maze task in rats. *European journal of anaesthesiology*. 2012;29 5:239-45; doi: 10.1097/EJA.0b013e32835103c1. <http://www.ncbi.nlm.nih.gov/pubmed/22343609>.
 14. Logan S, Pharaoh GA, Marlin MC, Masser DR, Matsuzaki S, Wronowski B, et al. Insulin-like growth factor receptor signaling regulates working memory, mitochondrial metabolism, and amyloid-beta

- uptake in astrocytes. *Molecular metabolism*. 2018;9:141-55; doi: 10.1016/j.molmet.2018.01.013. <http://www.ncbi.nlm.nih.gov/pubmed/29398615>.
15. Huang C, Zeng X, Jiang G, Liao X, Liu C, Li J, et al. XIAP BIR domain suppresses miR-200a expression and subsequently promotes EGFR protein translation and anchorage-independent growth of bladder cancer cell. *Journal of hematology & oncology*. 2017;10 1:6; doi: 10.1186/s13045-016-0376-9. <http://www.ncbi.nlm.nih.gov/pubmed/28057023>.
 16. Xinxing W, Hong F, Rui Z, Yun Z, Jingbo G, Lingjia Q. Phosphorylated nerve growth factor-induced clone B (NGFI-B) translocates from the nucleus to mitochondria of stressed rat cardiomyocytes and induces apoptosis. *Stress*. 2012;15 5:545-53; doi: 10.3109/10253890.2011.644603. <http://www.ncbi.nlm.nih.gov/pubmed/22128883>.
 17. La Sala L, Mrakic-Spota S, Tagliabue E, Prattichizzo F, Micheloni S, Sangalli E, et al. Circulating microRNA-21 is an early predictor of ROS-mediated damage in subjects with high risk of developing diabetes and in drug-naive T2D. *Cardiovascular diabetology*. 2019;18 1:18; doi: 10.1186/s12933-019-0824-2. <http://www.ncbi.nlm.nih.gov/pubmed/30803440>.
 18. Zhang Y, Xiao Y, Ma Y, Liang N, Liang Y, Lu C, et al. ROS-mediated miR-21-5p regulates the proliferation and apoptosis of Cr(VI)-exposed L02 hepatocytes via targeting PDCD4. *Ecotoxicology and environmental safety*. 2020;191:110160; doi: 10.1016/j.ecoenv.2019.110160. <http://www.ncbi.nlm.nih.gov/pubmed/31951899>.
 19. Mookerjee SA, Goncalves RLS, Gerencser AA, Nicholls DG, Brand MD. The contributions of respiration and glycolysis to extracellular acid production. *Biochimica et biophysica acta*. 2015;1847 2:171-81; doi: 10.1016/j.bbabi.2014.10.005. <http://www.ncbi.nlm.nih.gov/pubmed/25449966>.
 20. Obeidat YM, Cheng MH, Catandi G, Carnevale E, Chicco AJ, Chen TW. Design of a multi-sensor platform for integrating extracellular acidification rate with multi-metabolite flux measurement for small biological samples. *Biosensors & bioelectronics*. 2019;133:39-47; doi: 10.1016/j.bios.2019.02.069. <http://www.ncbi.nlm.nih.gov/pubmed/30909011>.
 21. Titone R, Robertson DM. Insulin receptor preserves mitochondrial function by binding VDAC1 in insulin insensitive mucosal epithelial cells. *FASEB journal : official publication of the Federation of American Societies for Experimental Biology*. 2020;34 1:754-75; doi: 10.1096/fj.201901316RR. <http://www.ncbi.nlm.nih.gov/pubmed/31914671>.
 22. Fabbri L, Dufies M, Lacas-Gervais S, Gardie B, Gad-Lapiteau S, Parola J, et al. Identification of a new aggressive axis driven by ciliogenesis and absence of VDAC1-DeltaC in clear cell Renal Cell Carcinoma patients. *Theranostics*. 2020;10 6:2696-713; doi: 10.7150/thno.41001. <http://www.ncbi.nlm.nih.gov/pubmed/32194829>.
 23. Ze X, Su M, Zhao X, Jiang H, Hong J, Yu X, et al. TiO2 nanoparticle-induced neurotoxicity may be involved in dysfunction of glutamate metabolism and its receptor expression in mice. *Environmental toxicology*. 2016;31 6:655-62; doi: 10.1002/tox.22077. <http://www.ncbi.nlm.nih.gov/pubmed/25411160>.

24. Song B, Zhang Y, Liu J, Feng X, Zhou T, Shao L. Unraveling the neurotoxicity of titanium dioxide nanoparticles: focusing on molecular mechanisms. *Beilstein journal of nanotechnology*. 2016;7:645-54; doi: 10.3762/bjnano.7.57. <http://www.ncbi.nlm.nih.gov/pubmed/27335754>.
25. Sheng L, Wang L, Su M, Zhao X, Hu R, Yu X, et al. Mechanism of TiO₂ nanoparticle-induced neurotoxicity in zebrafish (*Danio rerio*). *Environmental toxicology*. 2016;31 2:163-75; doi: 10.1002/tox.22031. <http://www.ncbi.nlm.nih.gov/pubmed/25059219>.
26. Shen C, Liu W, Zhang S, Pu L, Deng B, Zeng Q, et al. Downregulation of miR-541 induced by heat stress contributes to malignant transformation of human bronchial epithelial cells via HSP27. *Environmental research*. 2020;184:108954; doi: 10.1016/j.envres.2019.108954.
27. Huang R, Huang Y, Zeng G, Li M, Jin Y. Ursodeoxycholic acid inhibits intimal hyperplasia, vascular smooth muscle cell excessive proliferation, migration via blocking miR-21/PTEN/AKT/mTOR signaling pathway. *Cell cycle (Georgetown, Tex)*. 2020:1-15; doi: 10.1080/15384101.2020.1732514.
28. Chen J, Chen J, Cheng Y, Fu Y, Zhao H, Tang M, et al. Mesenchymal stem cell-derived exosomes protect beta cells against hypoxia-induced apoptosis via miR-21 by alleviating ER stress and inhibiting p38 MAPK phosphorylation. *Stem cell research & therapy*. 2020;11 1:97; doi: 10.1186/s13287-020-01610-0.
29. Jankovic N, Trifunovic Ristovski J, Vranes M, Tot A, Petronijevic J, Joksimovic N, et al. Discovery of the Biginelli hybrids as novel caspase-9 activators in apoptotic machines: Lipophilicity, molecular docking study, influence on angiogenesis gene and miR-21 expression levels. *Bioorganic chemistry*. 2019;86:569-82; doi: 10.1016/j.bioorg.2019.02.026.
30. Pan T, Jia P, Chen N, Fang Y, Liang Y, Guo M, et al. Delayed Remote Ischemic Preconditioning Confers Renoprotection against Septic Acute Kidney Injury via Exosomal miR-21. *Theranostics*. 2019;9 2:405-23; doi: 10.7150/thno.29832.
31. Li HJ, Pan YB, Sun ZL, Sun YY, Yang XT, Feng DF. Inhibition of miR-21 ameliorates excessive astrocyte activation and promotes axon regeneration following optic nerve crush. *Neuropharmacology*. 2018;137:33-49; doi: 10.1016/j.neuropharm.2018.04.028.
32. Guo NL, Zhang JX, Wu JP, Xu YH. Isoflurane promotes glucose metabolism through up-regulation of miR-21 and suppresses mitochondrial oxidative phosphorylation in ovarian cancer cells. *Bioscience reports*. 2017;37 6; doi: 10.1042/bsr20170818.
33. La Sala L, Mrakic-Spota S, Micheloni S, Prattichizzo F, Ceriello A. Glucose-sensing microRNA-21 disrupts ROS homeostasis and impairs antioxidant responses in cellular glucose variability. *Cardiovascular diabetology*. 2018;17 1:105; doi: 10.1186/s12933-018-0748-2.
34. Liu Y, Ren L, Liu W, Xiao Z. MiR-21 regulates the apoptosis of keloid fibroblasts by caspase-8 and the mitochondria-mediated apoptotic signaling pathway via targeting FasL. *Biochemistry and cell biology = Biochimie et biologie cellulaire*. 2018;96 5:548-55; doi: 10.1139/bcb-2017-0306.
35. Wu H, Wang J, Ma H, Xiao Z, Dong X. MicroRNA-21 inhibits mitochondria-mediated apoptosis in keloid. *Oncotarget*. 2017;8 54:92914-25; doi: 10.18632/oncotarget.21656.

36. Chowdhury SR, Djordjevic J, Albensi BC, Fernyhough P. Simultaneous evaluation of substrate-dependent oxygen consumption rates and mitochondrial membrane potential by TMRM and safranin in cortical mitochondria. *Bioscience reports*. 2015;36 1:e00286; doi: 10.1042/BSR20150244. <http://www.ncbi.nlm.nih.gov/pubmed/26647379>.
37. Kawashima H, Ozawa Y, Toda E, Homma K, Osada H, Narimatsu T, et al. Neuroprotective and vision-protective effect of preserving ATP levels by AMPK activator. *FASEB journal : official publication of the Federation of American Societies for Experimental Biology*. 2020;34 4:5016-26; doi: 10.1096/fj.201902387RR. <http://www.ncbi.nlm.nih.gov/pubmed/32090372>.
38. Stobart JL, Anderson CM. Multifunctional role of astrocytes as gatekeepers of neuronal energy supply. *Frontiers in cellular neuroscience*. 2013;7:38; doi: 10.3389/fncel.2013.00038.
39. Blachly-Dyson E, Forte M. VDAC channels. *IUBMB life*. 2001;52 3-5:113-8; doi: 10.1080/15216540152845902. <http://www.ncbi.nlm.nih.gov/pubmed/11798022>.
40. Shoshan-Barmatz V, Krelin Y, Chen Q. VDAC1 as a Player in Mitochondria-Mediated Apoptosis and Target for Modulating Apoptosis. *Current medicinal chemistry*. 2017;24 40:4435-46; doi: 10.2174/0929867324666170616105200. <http://www.ncbi.nlm.nih.gov/pubmed/28618997>.
41. Shoshan-Barmatz V, Nahon-Crystal E, Shteinfer-Kuzmine A, Gupta R. VDAC1, mitochondrial dysfunction, and Alzheimer's disease. *Pharmacological research*. 2018;131:87-101; doi: 10.1016/j.phrs.2018.03.010. <http://www.ncbi.nlm.nih.gov/pubmed/29551631>.
42. Arif T, Krelin Y, Nakdimon I, Benharroch D, Paul A, Dadon-Klein D, et al. VDAC1 is a molecular target in glioblastoma, with its depletion leading to reprogrammed metabolism and reversed oncogenic properties. *Neuro-oncology*. 2017;19 7:951-64; doi: 10.1093/neuonc/now297.
43. Zhang E, Mohammed Al-Amily I, Mohammed S, Luan C, Asplund O, Ahmed M, et al. Preserving Insulin Secretion in Diabetes by Inhibiting VDAC1 Overexpression and Surface Translocation in beta Cells. *Cell metabolism*. 2019;29 1:64-77.e6; doi: 10.1016/j.cmet.2018.09.008.
44. Yang G, Zhou D, Li J, Wang W, Zhong W, Fan W, et al. VDAC1 is regulated by BRD4 and contributes to JQ1 resistance in breast cancer. *Oncology letters*. 2019;18 3:2340-7; doi: 10.3892/ol.2019.10534.

Figures

Figure 1

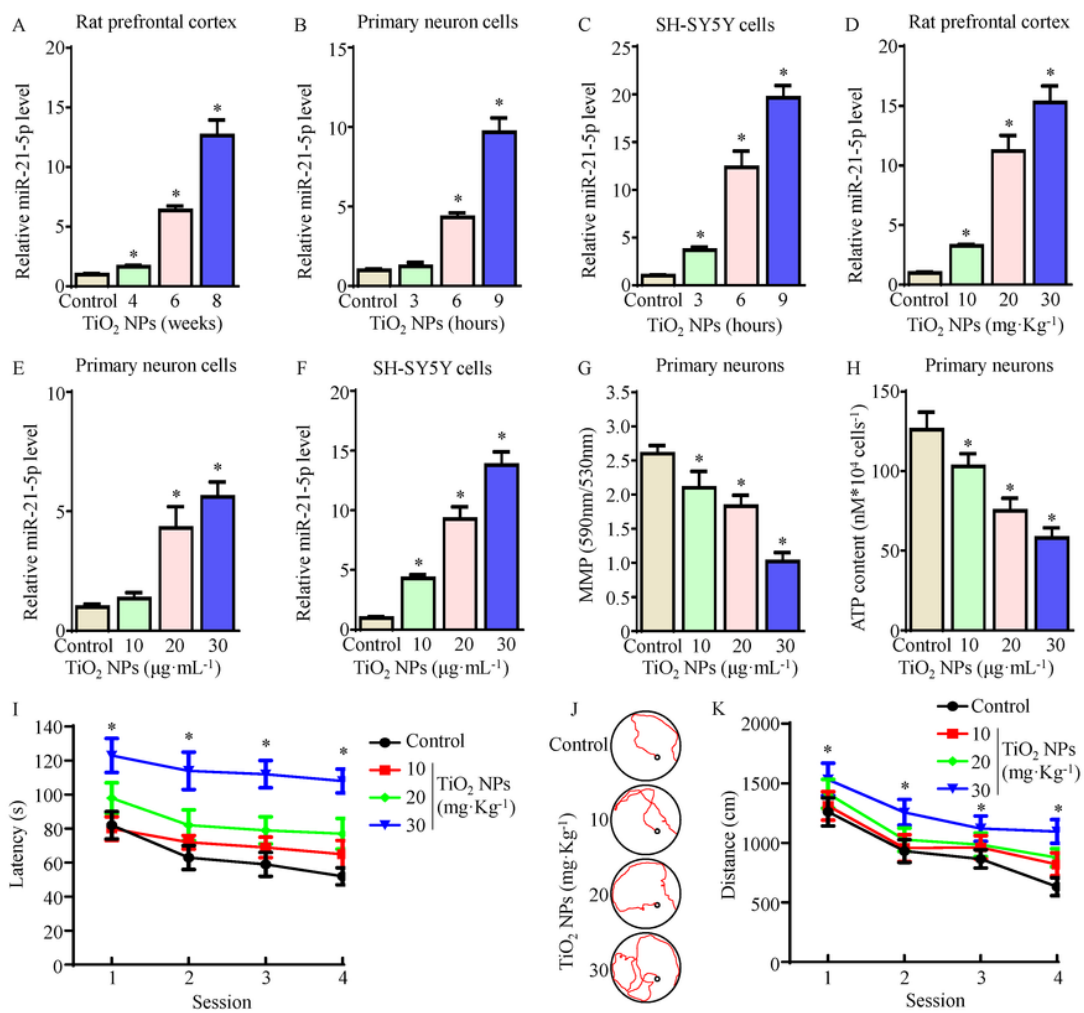


Figure 1

TiO₂ NPs led to cognitive deficits, mitochondrial dysfunction, and upregulation of miR-21-5P. (A) Wistar rats (six rats in each group) were exposed to 20 mg·Kg⁻¹ TiO₂ NPs for 4, 6, or 8 weeks. The extracts of prefrontal cortex tissue were subjected to RT-PCR to determine miR-21-5P expression. Gapdh was used as an internal reference. (B-C) Primary neuron cells or SH-SY5Y cells were seeded into wells of 6-well plates and cultured until the cell density reached 80-90%. The cells were then exposed to 20 μg·mL⁻¹ TiO₂ NPs for 3, 6, or 9 hours. The extracts were subjected to RT-PCR to determine miR-21-5P expression. Gapdh/GAPDH was used as an internal reference. (D) Wistar rats (six rats in each group) were exposed to 10, 20, or 30 mg·Kg⁻¹ TiO₂ NPs for 8 weeks. The extracts of prefrontal cortex tissue were subjected to RT-PCR to determine miR-21-5P expression. Gapdh was used as an internal reference. (E-F) Primary neuron cells or SH-SY5Y cells were exposed to 10, 20, or 30 μg·mL⁻¹ TiO₂ NPs for 9 hours. The extracts were subjected to RT-PCR to determine miR-21-5P expression. Gapdh/GAPDH was used as an internal reference. (G) Primary neuron cells were treated with 10, 20, or 30 μg·mL⁻¹ TiO₂ NPs for 9 hours. Changes in the mean JC-1 fluorescence ratio (590 nm/530 nm) of cells were detected to indicate the ΔΨ_m. (H) Primary neuron cells were treated with 10, 20, or 30 μg·mL⁻¹ TiO₂ NPs for 9 hours. The cell extracts were

subjected to HPLC to determine the ATP levels. (I-K) Wistar rats (six rats in each group) were exposed to 10, 20, or 30 mg·Kg⁻¹ TiO₂ NPs for 8 weeks and sent to water maze test. The symbol (*) indicates a significant increase in comparison with that of the control (P < 0.05).

Figure 2

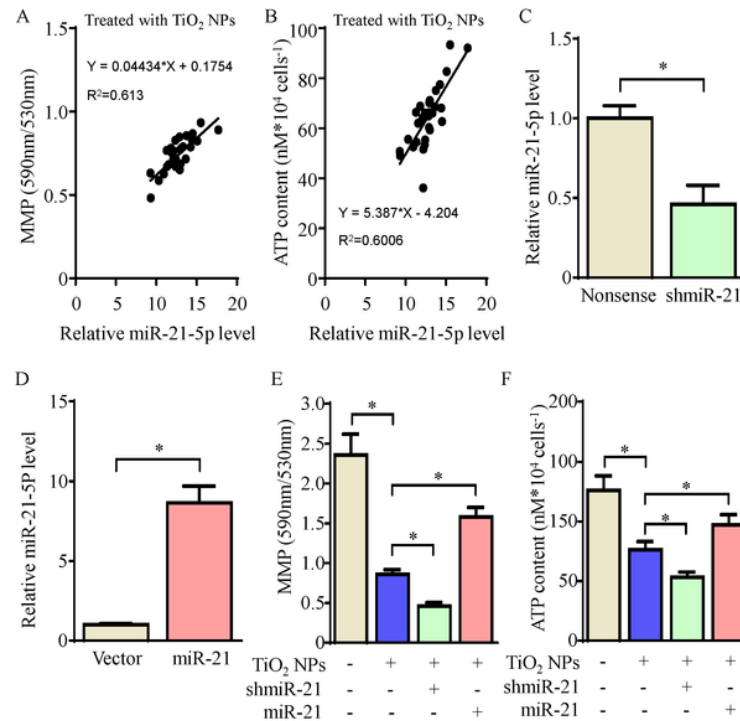


Figure 2

MiR-21-5p preserved the mitochondrial membrane potential ($\Delta\Psi_m$) and ATP levels of SH-SY5Y cells under TiO₂ NP treatment. (A) SH-SY5 cells were seeded into wells of 6-well plates and cultured until the cell density reached 80–90%. The cells were then exposed to 20 $\mu\text{g}\cdot\text{mL}^{-1}$ TiO₂ NPs for 9 hours. Some of the cells were collected for $\Delta\Psi_m$ detection and some for RT-PCR in the same group. (B) SH-SY5 cells were seeded into wells of 6-well plates and cultured until the cell density reached 80–90%. The cells were then exposed to 20 $\mu\text{g}\cdot\text{mL}^{-1}$ TiO₂ NPs for 9 hours. Some of the cells were collected for ATP detection and some for RT-PCR in the same group. (C) MiR-21-5p knockdown was identified in SH-SY5 cells (shmiR-21-5p) in comparison with control SH-SY5 cells (Nonsense). The symbol (*) indicates a significant decrease in comparison with that of the nonsense group (P < 0.05). (D) MiR-21-5p overexpression was identified in SH-SY5 cells (miR-21-5p) in comparison with control SH-SY5 cells (Vector). The symbol (*) indicates a significant increase in comparison with that of the vector group (P < 0.05). (E) SH-SY5 cells, SH-SY5 cells

(shmiR-21-5p), or SH-SY5 cells (miR-21-5p) were treated with or without 20 $\mu\text{g}\cdot\text{mL}^{-1}$ TiO₂ NPs for 9 hours. The cells were then subjected to $\Delta\Psi\text{m}$ detection. The symbol (*) indicates a significant change in comparison between marked groups ($P < 0.05$). (F) SH-SY5 cells, SH-SY5 cells (shmiR-21-5p), or SH-SY5 cells (miR-21-5p) were treated with or without 20 $\mu\text{g}\cdot\text{mL}^{-1}$ TiO₂ NPs for 9 hours. The cells were then subjected to ATP detection. The symbol (*) indicates a significant change in comparison between marked groups ($P < 0.05$).

Figure 3

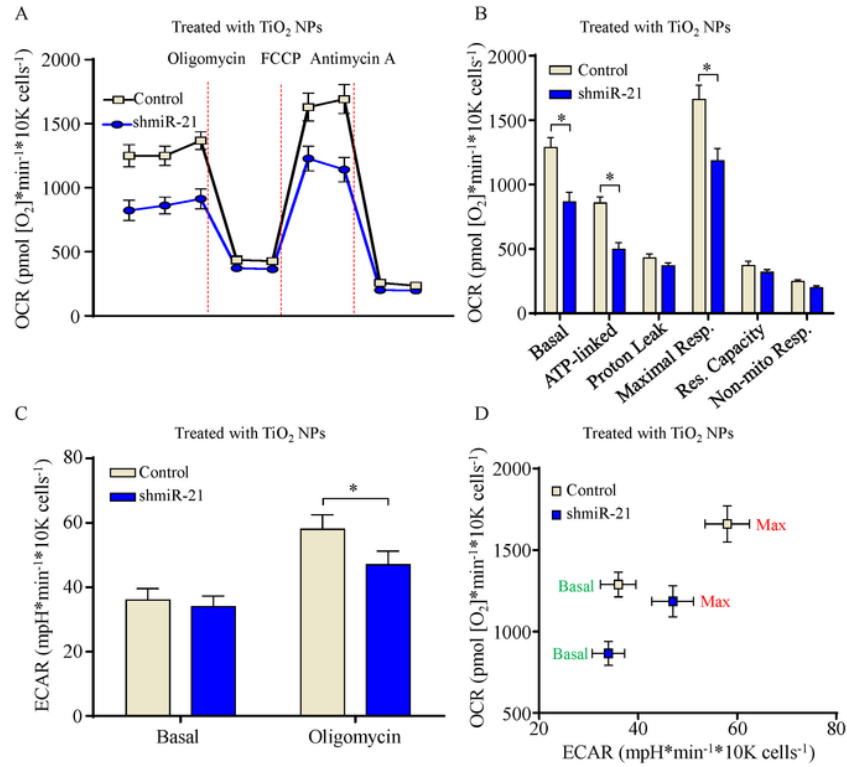


Figure 3

MiR-21-5p knockdown decreased maximal respiration in SH-SY5 cells treated with TiO₂ NPs. (A) SH-SY5 cells (Control) or SH-SY5 cells (shmiR-21-5p) were treated with 20 $\mu\text{g}\cdot\text{mL}^{-1}$ TiO₂ NPs for 9 hours and then subjected to Seahorse system analysis to determine the oxygen consumption rate (OCR). (B) Quantitative analysis of (A). The symbol (*) indicates a significant decrease in comparison with that of the control ($P < 0.05$). (C) SH-SY5 cells (Control) or SH-SY5 cells (shmiR-21-5p) were treated with 20 $\mu\text{g}\cdot\text{mL}^{-1}$ TiO₂ NPs for 9 hours and then subjected to Seahorse system analysis to determine oligomycin-induced extracellular acidification rate (ECAR). (D) Basal and maximal OCR to ECAR ratios were calculated to

indicate the induction of a response to FCCP in SH-SY5 cells (shmiR-21-5p) compared with that in the control.

Figure 4

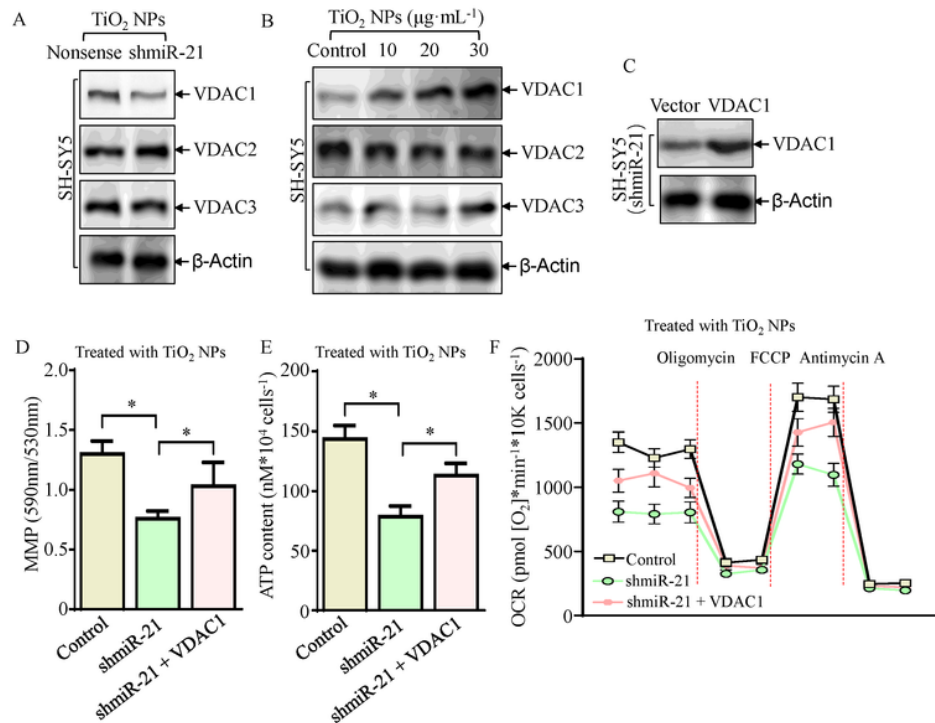


Figure 4

VDAC1 was crucial for miR-21-5p to protect the mitochondria function of TiO₂ NP-treated SH-SY5 cells. (A) SH-SY5 cells (Nonsense) and SH-SY5 cells (shmiR-21-5p) were treated with 20 µg·mL⁻¹ TiO₂ NPs for 9 hours. The cell extracts were subjected to western blotting to determine the VDAC1, VDAC2, and VDAC3 levels. β-Actin was used as a protein loading control. (B) SH-SY5 cells were exposed to 10, 20, or 30 µg·mL⁻¹ TiO₂ NPs for 9 hours. The cell extracts were subjected to western blotting to determine the VDAC1, VDAC2, and VDAC3 levels. β-Actin was used as a protein loading control. (C) VDAC1 overexpression was identified in SH-SY5 cells (shmiR-21, VDAC1) in comparison with control SH-SY5 cells (shmiR-21, vector). (D) SH-SY5 cells (Nonsense), SH-SY5 cells (shmiR-21), and SH-SY5 cells (shmiR-21, VDAC1) were treated with 20 µg·mL⁻¹ TiO₂ NPs for 9 hours. Changes in the mean JC-1 fluorescence ratio (590 nm/530 nm) of cells were detected to indicate the ΔΨ_m levels. (E) SH-SY5 cells (Nonsense), SH-SY5 cells (shmiR-21-5p), and SH-SY5 cells (shmiR-21-5p, VDAC1) were treated with 20 µg·mL⁻¹ TiO₂ NPs for 9 hours. The cell extracts were subjected to HPLC to determine the ATP levels. (F) SH-SY5 cells

(Nonsense), SH-SY5 cells (shmiR-21-5p), and SH-SY5 cells (shmiR-21-5p, VDAC1) were treated with 20 $\mu\text{g}\cdot\text{mL}^{-1}$ TiO₂ NPs for 9 hours. The cells were analyzed using the Seahorse system to determine the OCR.

Figure 5

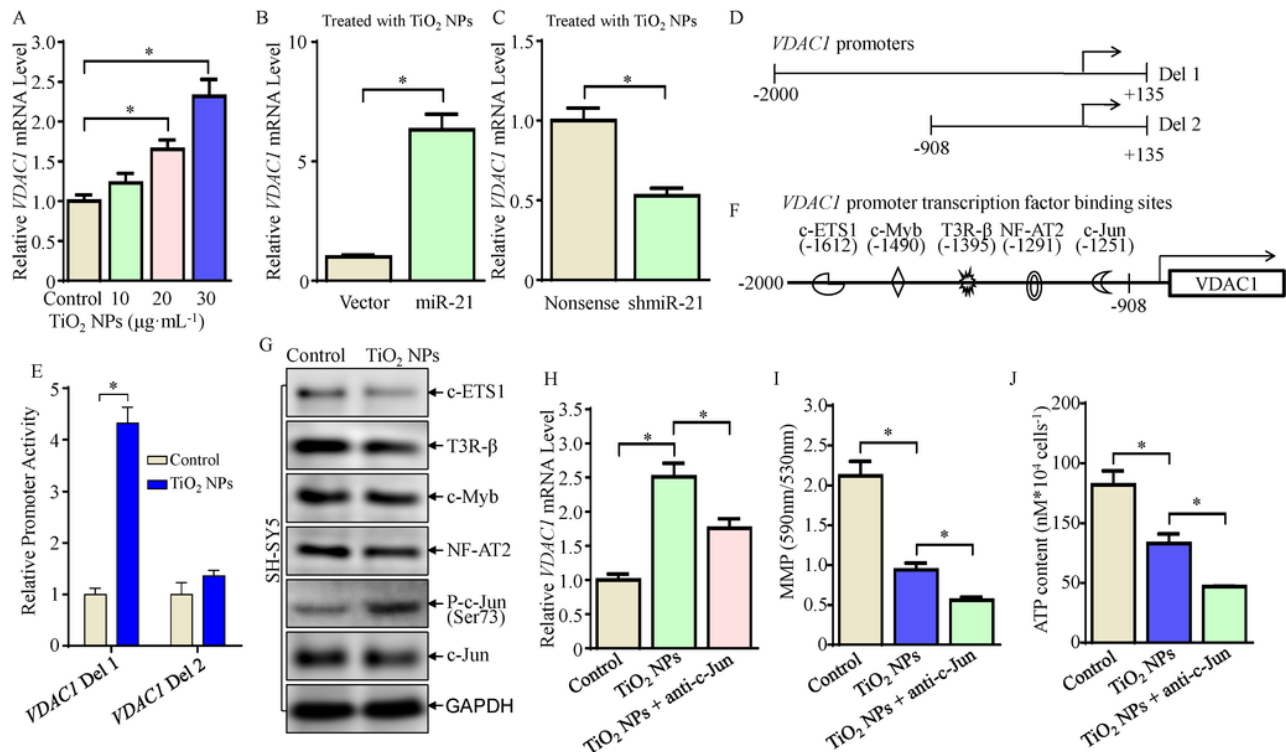


Figure 5

Phosphorylated c-Jun was responsible for upregulation of VDAC1 in TiO₂ NP-treated SH-SY5 cells. (A) SH-SY5 cells were exposed to 10, 20, or 30 $\mu\text{g}\cdot\text{mL}^{-1}$ TiO₂ NPs for 9 hours. The cell extracts were subjected to RT-PCR to determine VDAC1 mRNA expression. GAPDH was used as an internal reference. (B) SH-SY5 cells (Vector) and SH-SY5 cells (miR-21-5p) were treated with 20 $\mu\text{g}\cdot\text{mL}^{-1}$ TiO₂ NPs for 9 hours. The cell extracts were subjected to RT-PCR to determine VDAC1 mRNA expression. GAPDH was used as an internal reference. (C) SH-SY5 cells (Nonsense) and SH-SY5 cells (shmiR-21-5p) were treated with 20 $\mu\text{g}\cdot\text{mL}^{-1}$ TiO₂ NPs for 9 hours. The cell extracts were subjected to RT-PCR to determine VDAC1 mRNA expression. GAPDH was used as an internal reference. The symbol (*) indicates a significant increase in comparison with that of the control ($P < 0.05$). (D) Schematic illustration of the construction of the VDAC1 promoter-driven luciferase reporter constructs. (E) The VDAC1 promoter-driven luciferase reporter constructs co-transfected with TK into H9c2 cells, with or without exposure to 20 $\mu\text{g}\cdot\text{mL}^{-1}$ TiO₂ NPs for 9 hours, respectively. The luciferase activity of the transfectants was evaluated after 24 h, and

the results are presented as relative VDAC1 promoter activity by normalization to TK and pGL3, respectively. The symbol (*) indicates a significant increase in comparison with the that of the control ($P < 0.05$). (F) Potential transcription factor binding sites in the VDAC1 promoter region (-2000 ~ -908) were analyzed using the TRANSFAC 8.3 engine online. (G) SH-SY5 cells were treated with $20 \mu\text{g}\cdot\text{mL}^{-1}$ TiO₂ NPs for 9 hours. The cell extracts were analyzed for the levels of potential transcription factors of VDAC1 using western blotting. (H-J) SH-SY5 cells and SH-SY5 cells (anti-c-Jun) were treated with 1% O₂ for 6 hours. The cell extracts were analyzed for the levels of VDAC1 mRNA and ATP content. Changes in the mean JC-1 fluorescence ratio (590 nm/530 nm) of cells were detected to indicate the $\Delta\Psi\text{m}$ levels.

Supplementary Files

This is a list of supplementary files associated with this preprint. Click to download.

- [SupplementalInformation.docx](#)
- [OnlineGraphicalabstract.png](#)